東シナ海における黒潮の数日間の変化

Mem. Fac. Fish. Kagoshima Univ.,
Vol. 46, pp. 11~20 (1997)

Temporal Change of the Kuroshio in the East China Sea During Several Days

Hirohiko Nakamura*[1], Hiroshi Ichikawa*[1], Masaaki Chaen*[1],
Kiyoshi Shimada*[2], Masaki Uchiyama*[2] and Keisuke Yoshinaga*[2]

Keywords : The Kuroshio axis, The Kuroshio front, Temporal change

Abstract

In order to examine temporal changes of the Kuroshio, the observation was carried out twice on March 1-4 and March 7-10, 1997 along three sections across the Kuroshio in the East China Sea by T/V Keitenmaru of Kagoshima University. Two of these sections were located in the continental slope region and one in the Tokara Strait.

Horizontal shifts of the surface temperature front (hereafter, called the Kuroshio front) were closely related to those of the position of the maximum surface velocity (hereafter, called the Kuroshio axis) in all cross-sections. However, the former varied with a several times (1.8~7) larger amplitude than the latter. The Kuroshio in the Tokara Strait was focused on, because the Kuroshio axis shifted northward with the large distance of 60km during 8 days. The vertical structure of the Kuroshio in the strait was characterized by the upper- and lower-interfaces. The maximum tilt of the lower-interface geographically corresponded to the Kuroshio axis. On the other hand, the outcropping of the upper-interface corresponded to the Kuroshio front. Since the structure of the lower-interface changed little during the northward migration of the Kuroshio, the surface velocity at the Kuroshio axis was maintained. The structure of the upper-interface changed significantly, and this resulted in the horizontal shift of the Kuroshio front with a twice larger amplitude than the Kuroshio axis. These observations suggest that the fluctuation of the Kuroshio axis is dynamically different from that of the Kuroshio front.

It is well known that the Kuroshio in the East China Sea (ECS) varies with several periods between a few days and a few months. Most of the previous studies on the variability of the Kuroshio are classified into two groups. One group focuses on variations of the position of the maximum surface velocity, which is generally called the Kuroshio axis (e.g., Yamashiro et al.[1]; Yamashiro and Kawabe[2]) and the other on those of the surface temperature front, which is generally called the Kuroshio front (e.g., Qiu et al.[3]; Akiyama and Ameya[4]). However, the relationship between two groups is not studied except for Maeda et al.[5]. Using sea level data and sea surface temperature acquired by a ferryboat, they showed that the northward migration of the Kuroshio front decreases the transport in the southern strait between Naze and Nakano-shima, but increases in the northern strait between Nakano-shima and Sata-misaki. This suggests that the northward migration of the Kuroshio front in the Tokara Strait synchronizes with that of the Kuroshio axis. However, physical aspects of the relationship between them, such as phase speeds and growing rates, have been unclear. A primary objective of this study is to examine the precise relationship between the variation of the position of the Kuroshio axis and that of the Kuroshio front from analyzing changes of temperature and current structures in cross-sections

*[1]Division of Environmental and Information Sciences, Faculty of Fisheries, Kagoshima University, 50-20 Shimoarata 4, Kagoshima, 890 Japan

*[2]T/V Keitenmaru, Faculty of Fisheries, Kagoshima University, 50-20 Shimoarata 4, Kagoshima, 890 Japan

during several days.

This paper is arranged as follows: An outline of the observation is mentioned in section 2. All cross-sections of temperature, salinity, ADCP velocity and absolute geostrophic velocity are presented and discussed in section 3. The relationship between the variation of the position of the Kuroshio axis and that of the Kuroshio front at three cross-sections is presented in section 4. The change of the temperature cross-section in the Tokara Strait is focused on in section 5. In section 6, we summarize observed results.

Observation

Hydrographic observations with the XBT, CTD with RMS, and current observation with the shipboard ADCP were carried out along three sections across the Kuroshio in the ECS by T/V Keitenmaru of Kagoshima University. The observation was

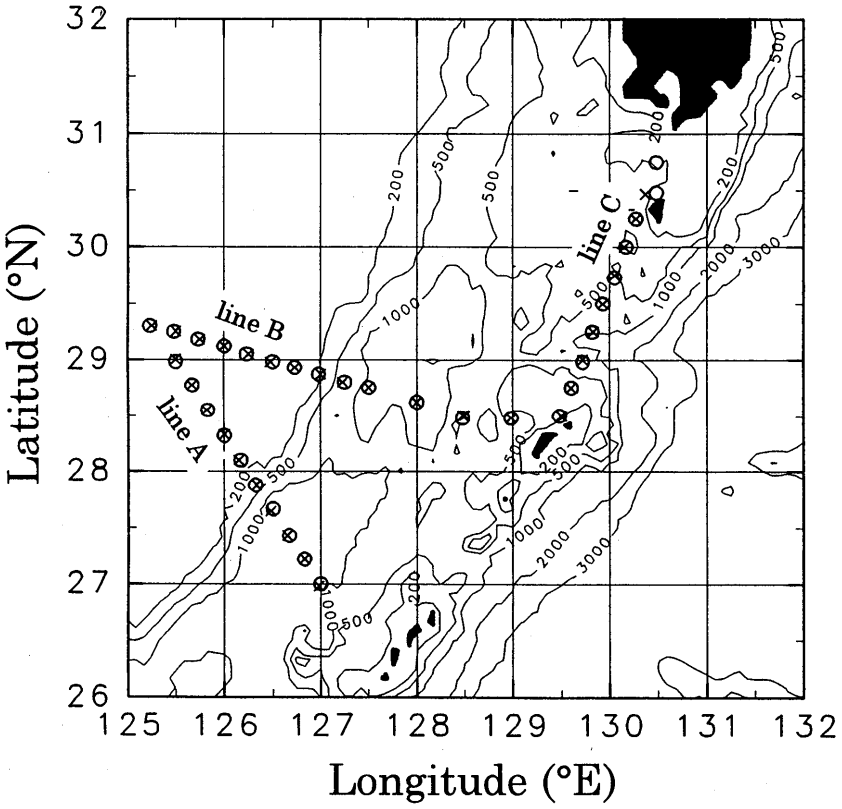

Fig. 1 Map of the study area in the East China Sea, showing the XBT stations (crosses) and CTD stations (circles). Data of bottom topography are the Terrain Base Global Land and Ocean Depth (5×5 min) provided by the National Geophysical Data Center.

Table 1 Survey period (UTC) and time interval between leg. 1 and leg. 2

leg. 1	Line A	Line B	Line C
Start	23:39, March 3, 1997	08:04, March 3, 1997	12:14, March 1, 1997
End	17:40, March 4, 1997	23:39, March 3, 1997	04:51, March 2, 1997
Mean	08:40, March 4, 1997	15:52, March 3, 1997	20:33, March 1, 1997
leg. 2	Line A	Line B	Line C
Start	10:24, March 7, 1997	08:52, March 8, 1997	13:50, March 9, 1997
End	08:52, March 8, 1997	06:31, March 9, 1997	08:44, March 10, 1997
Mean	21:43, March 7, 1997	20:33, March 8, 1997	23:07, March 9, 1997
	Line A	Line B	Line C
Time interval	~3.5 days	~5 days	~8 days

performed twice (leg. 1 and leg. 2) along the same lines shown in Fig. 1. Hereafter, each line is called line A (between Okinawa and the continental shelf), line B (between Amami-oushima and the continental shelf) and line C (across the Tokara Strait). The hydrographic casts with XBT (basically to 750m) were performed in leg. 1 during March 1-4 (UTC), 1997, and the CTD observations (to the bottom, but 1500-m depth if the bottom is shallower than 1500-m depth) were performed in leg. 2 during March 7-10, 1997. Current data with ADCP were obtained basically at 5-m, 50-m and 100-m depths with every one-minute interval over leg. 1 and every 30-minute interval over leg. 2. The coarse ADCP sampling in leg. 2 was due to the bad condition of the recording system of GPS data. Date and time of the observation at each line are summarized in Table 1.

Temperature, salinity, ADCP velocity and absolute geostrophic velocity

Data processing

XBT data are arranged in every 5-m interval by using a gausian filter with the 5-m e-falling scale, after removing unusual values over 3 σ to mean values averaged within every 10-m interval. XBT temperature distributions (leg. 1) processed by the 25-m running mean along line A, line B and Line C are presented in Fig. 2.

CTD salinity data were calibrated through the following processes: The conductivity measured by CTD was corrected by comparing salinity of 64 bottle samples at specific depths on the upcast with the CTD determined values. Samples were analyzed with the AUTOSAL 8400B salinometer, referenced to the IAPSO standard sea water (batch number, P127). The best quadric coefficients to make CTD salinity equal to bottle salinity were determined by the least square method for 51 salinity data. The standard deviation of corrected CTD salinity from bottle salinity was 0.0027psu. CTD temperature and salinity are arranged in every 1-m interval, adopting the method that decreases the number of density inversions caused by the difference of response times between temperature and conductivity sensors. CTD

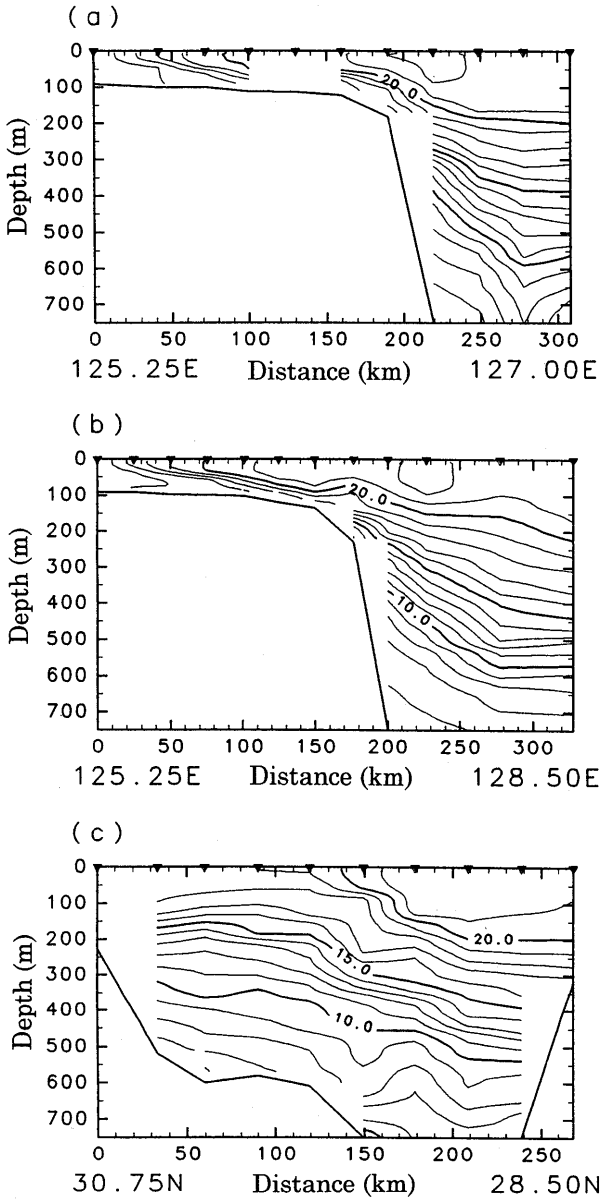

Fig. 2 Cross-sections of temperature in leg. 1 along (a) line A, (b) line B, and (c) line C. Contour interval is 1.0 ℃.

temperature and salinity distributions (leg. 2) processed by the 25-m running mean along line A, line B, line C are presented in Fig. 3 and Fig. 4, respectively.

Thirty-minute mean absolute velocity of ADCP is calculated at 5-m, 50-m and 100-m depths as a vector sum of the detected Doppler velocity and the ship velocity. Horizontal distributions of ADCP velocity at 5-m depth in leg. 1 and leg. 2 are presented in Fig. 5a and Fig. 5b, respectively.

The absolute geostrophic velocity, using ADCP velocity at 5-m depth as the reference level velocity,

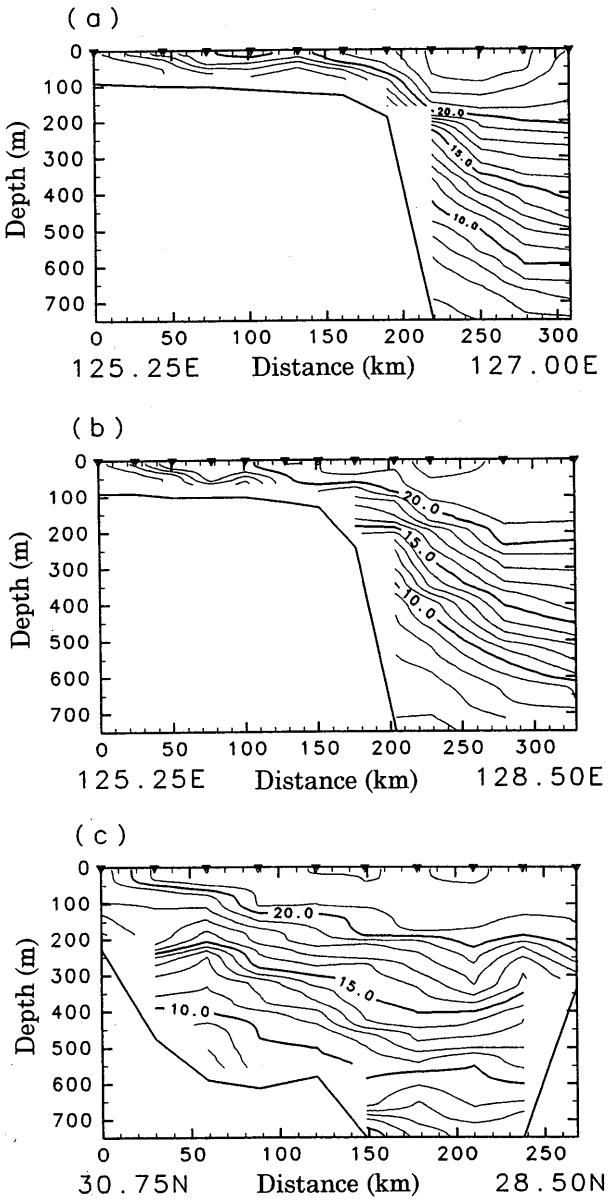

Fig. 3 Cross-sections of temperature in leg. 2 along (a) line A, (b) line B, and (c) line C. Contour interval is 1.0 ℃.

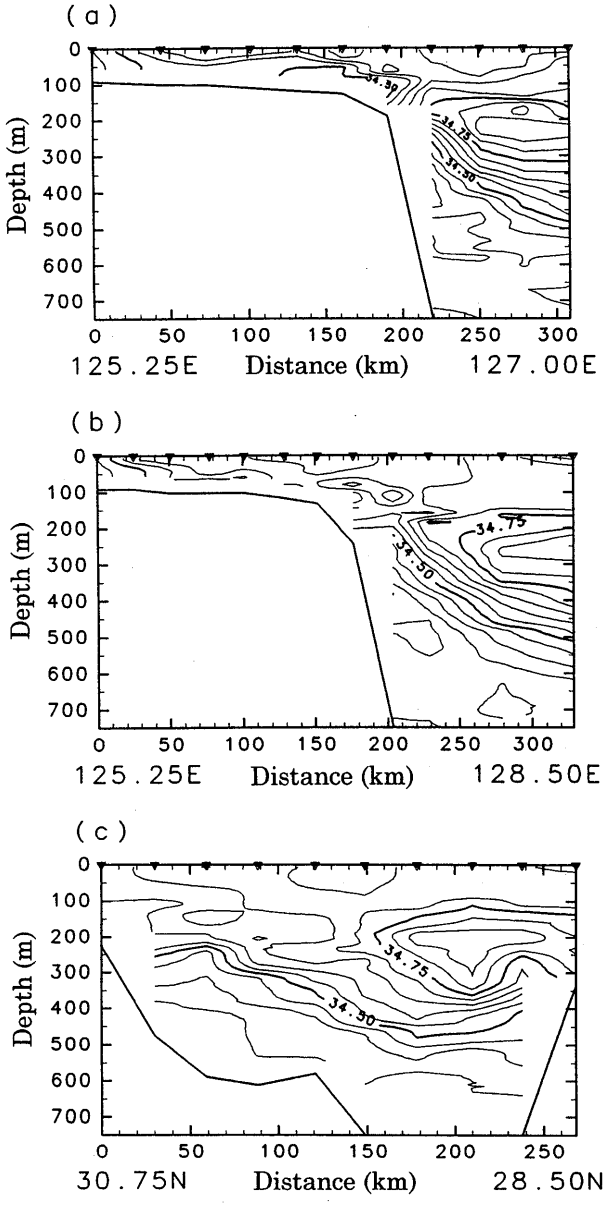

Fig. 4 Cross-sections of salinity in leg. 2 along (a) line A, (b) line B, and (c) line C. Contour interval is 0.005psu.

is simply calculated in all lines of leg. 2. ADCP data may include ageostrophic components, such as barotropic and baroclinic tides, but these components are not removed in this preliminary analysis. Distributions of the absolute geostrophic velocity (leg. 2) along line A, line B and line C are presented in Fig. 6.

Distributions

Cross-sections of temperature (Fig. 3), salinity (Fig. 4) and absolute geostrophic velocity (Fig. 6) in leg. 2 are discussed, because both temperature and salinity were observed with CTD in leg. 2.

On line A, a shelf water characterized by low temperature ($\leq$ 17.0 ℃) and low salinity ($\leq$ 34.50psu) existed on the continental shelf edge. As a result, a sharp salinity front between the shelf water and the Kuroshio saline water ($\geq$ 34.75psu) was formed at 100-m depth on the continental shelf edge. A shelf water ($\leq$17.0℃ and $\leq$34.50psu) on line B existed at the more western side than on line A. The Kuroshio subsurface water characterized by a

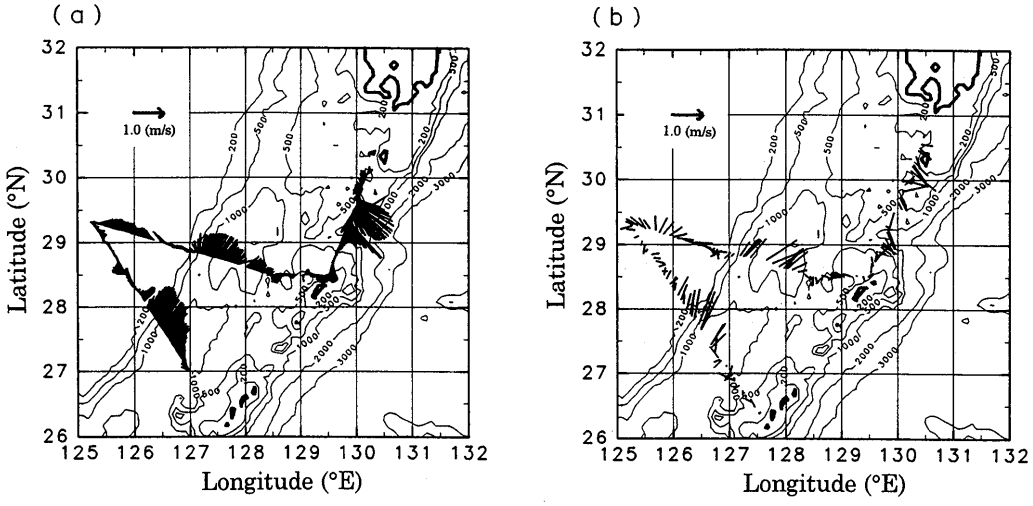

Fig. 5 Horizontal distributions of ADCP velocity at 5-m depth (a) in leg. 1 and (b) in leg. 2. Sticks in (a) are drawn with every 5-minute interval, while these in (b) with every 30-minute interval.

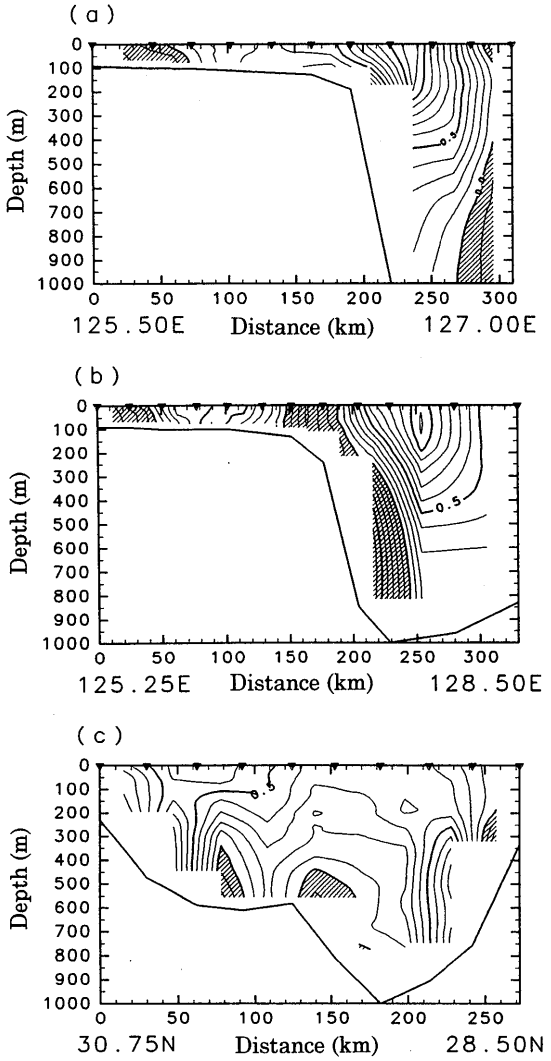

Fig. 6 Cross-sections of absolute geostrophic velocity in leg. 2 along (a) line A, (b) line B, and (c) line C. Contour interval is 0.1m/s. Hatched area indicates negative velocity. Velocity convention: the current direction of the Kuroshio is positive.

vertical homogeneity covered over the continental shelf region within about 50km west of the continental slope. On line C, the shelf water with the same characteristic as on the continental slope ($\leq$17.0℃ and $\leq$34.50psu) did not appear.

The maximum northward velocity on line A was higher than 1.0m/s at the sea surface on the continental slope. On line B, the maximum northward velocity was 1.1m/s at 75-m depth on the off-shore side away from the continental slope and the southward flow with the higher speed than 0.5m/s existed under the northward Kuroshio current on the continental slope. Comparing line A with line B, the Kuroshio axis was closer to the continental slope on line A than on line B. The maximum velocity on line C was approximately 0.6m/s at the sea surface around 30° N. Several cores of the minimum velocity existed near the bottom on this line. These complex features may be caused by the ageostrophic components which are included in both ADCP data and hydrographic data.

The high salinity core of the Kuroshio ($\geq$ 34.75psu) was placed just east of the Kuroshio axis identified by the maximum velocity on both line A and line B. However, the high salinity core on line C lay about 100km south of the Kuroshio axis.

Temporal changes of the Kuroshio axis and the Kuroshio front

In order to examine the relationship between the variation of the position of the Kuroshio axis and that of the Kuroshio front, both ADCP surface velocity profiles and temperature cross-sections are analyzed. The position of the Kuroshio axis is detected by the maximum ADCP velocity at 5-m depth perpendicular to each line. The Kuroshio front is regarded as an outcropped line of 20℃ isotherm in this paper. The outcropped line of 20℃ isotherm has a good correspondence to the on-shore edge of the subsurface warm water of the Kuroshio (see Fig. 2 and Fig. 3), so that its variation indicates the horizontal shift of the subsurface warm water. The actual temperature front should be determined by the largest horizontal temperature gradient at the sea surface. The outcropped line of 20℃ isotherm is compared with the temperature front determined by the temperature gradient.

Figures 7 and 8 show the profiles of normal velocity components at 5-m depth on each line in leg. 1 and leg. 2, respectively. Positions of the Kuroshio axis are indicated in these figures with the interpolation in the area where ADCP velocity data lack. Positions of the Kuroshio front are also indicated in

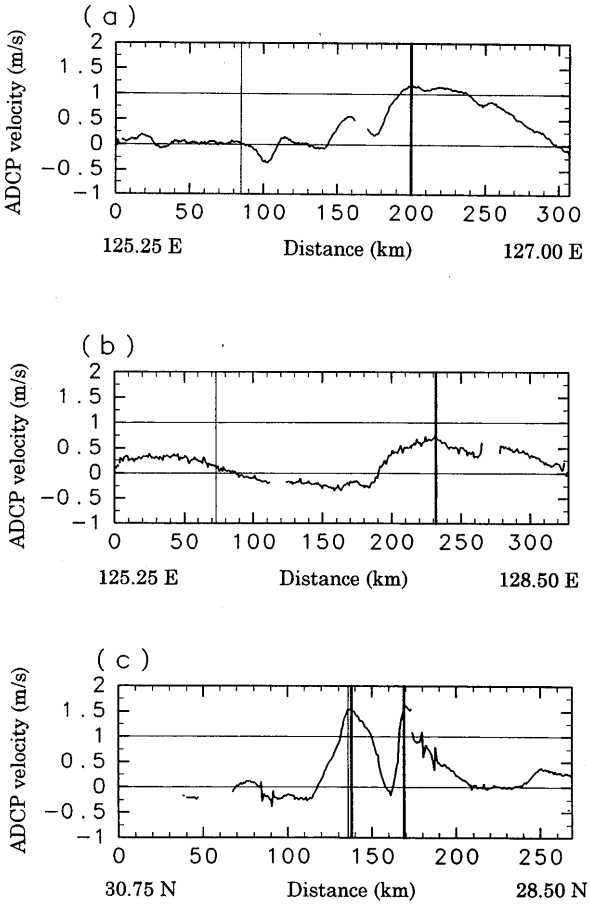

Fig. 7 ADCP velocity at 5-m depth perpendicular to the observed lines in leg. 1 along (a) line A, (b) line B, and (c) line C. Vertical bold solid line indicates position of the Kuroshio axis detected by the maximum ADCP velocity. Vertical thin solid line indicates position of the Kuroshio front detected by the outcropped line of 20℃ isotherm.

Table 2 Displacements of the Kuroshio axis detected by the maximum ADCP velocity and the Kuroshio front detected by the outcropped line of 20℃ isotherm. Plus sign indicates the displacement to the off-shore side, while minus sign to the on-shore side.

	Kuroshio axis (km)	Kuroshio front (km)
Line A	+8	+57
Line B	+20	+35
Line C	−58 (for the northern axis) −59 (for the southern axis)	−118

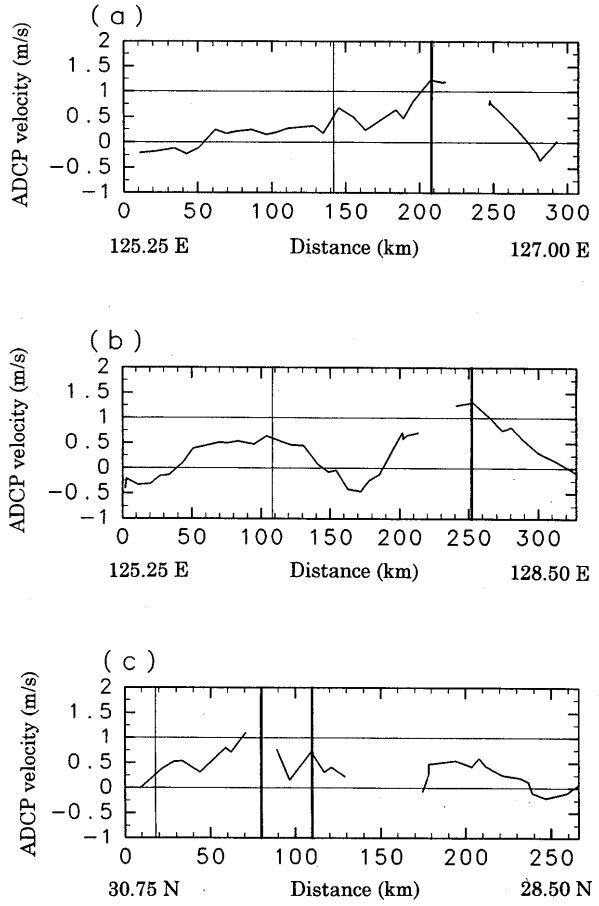

Fig. 8 Same as in Fig. 7, except leg. 2.

these figures, extracting 20℃ outcropped line from temperature cross-sections (Fig. 2 and Fig. 3). Table 2 summarizes displacements of these characteristics between leg. 1 and leg. 2.

line A

Observations along line A were performed with the interval of about 3.5 days. Maximum ADCP velocities (Fig. 7a and Fig. 8a) show that the Kuroshio axis shifted eastward with a distance of 8km. The structure of the subsurface warm water was significantly different between leg. 1 and leg. 2 (Fig. 2a and Fig. 3a). The Kuroshio front moved eastward with a distance of 57km, detaching a warm water patch from the Kuroshio front. The subsurface warm water east of the continental slope was about 1℃ warmer in leg. 2 than in leg. 1. Actual surface temperature fronts in both leg. 1 and leg. 2 are identified by 16-19 ℃ isotherms with the largest temperature gradient at the sea surface. This front is also identified as the salinity front in leg. 2 (Fig. 4a), so that this can be regarded as the water-mass front between the Kuroshio water and the shelf water. The water mass front did not move during 3.5 days. The Kuroshio front shifted with about 7 times longer distance than the Kuroshio axis.

line B

Observations along line B were performed with the interval of about 5 days. Maximum ADCP velocities (Fig. 7b and Fig. 8b) show that the Kuroshio axis shifted eastward with a distance of 20km. On the other hand, the Kuroshio front moved eastward with a distance of 35km. On this line, the Kuroshio front shifted with about 1.8 times longer distance than the Kuroshio axis. As seen on line A, the water-mass front in line B is identified by 16-19℃ isotherms in both leg. 1 and leg. 2. This did not move during 5 days.

line C

Observations along line C were performed with the interval of about 8 days. The distribution of ADCP velocity in leg. 1 (Fig. 7c) shows two apparent maximums with the higher speed than 1.0m/s. That in leg. 2 (Fig. 8c) also shows two maximums around 30° N, although the southern one is weakened under 1.0m/s and a peak of the northern one disappears owing to the lack of data. Both northern and southern maximums in leg. 1 shifted northward with the same distance of about 60km. On the other hand, the Kuroshio front moved northward with a distance of 118km. On this line, the actual surface temperature front with the sharp temperature gradient at the sea surface corresponds to the Kuroshio front identified by the outcropped line of 20 ℃ isotherm. The Kuroshio front shifted with about twice longer distance than the Kuroshio axis.

Change of temperature structure in the Tokara Strait

The horizontal shifts of both the Kuroshio axis and the Kuroshio front were larger in the Tokara Strait than in the other cross-sections. Thus, we could

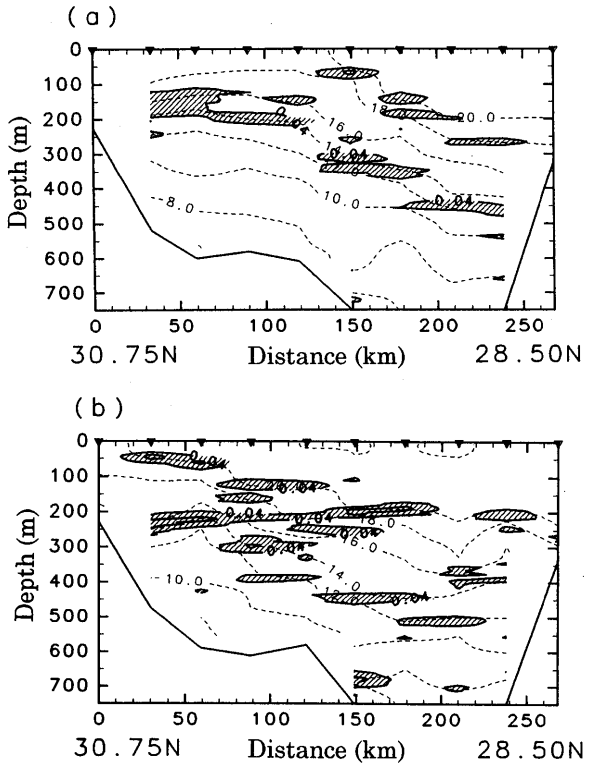

Fig. 9 Cross-sections of vertical temperature gradient along line C (a) in leg. 1 and (b) in leg. 2. The vertical temperature gradient larger than 0.04℃/m is hatched. Temperature distribution (dashed line) is superimposed in (a) and (b). Contour interval is 2.0℃.

precisely analyze the change of the Kuroshio structure in the Tokara strait. Our interest in the analysis is the change of the baroclinic structure caused by the horizontal shift of the Kuroshio.

The vertical structure of the Kuroshio in the cross-section is firstly characterized by the distribution of the vertical temperature gradient. Figures 9a and 9b show the distribution of the vertical temperature gradient larger than 0.04℃/m in leg. 1 and leg. 2, respectively. These figures indicate that the Kuroshio in the Tokara strait is vertically separated by two interfaces corresponding to layers with the large vertical temperature gradient: one interface (upper-interface) is approximately formed around 18 -20℃ isotherms, and the other (lower-interface) around 12-14℃ isotherms in the southern strait while 14-16℃ isotherms in the northern strait. Three layers separated by these interfaces are characterized by 1) the subsurface warm water warmer than 20℃ (upper-layer), 2) the upper part of the main thermocline between 14-18℃ isotherms (middle-layer), which corresponds to the characteristic temperature of the Subtropical Mode Water, and 3) the lower part of the main thermocline (lower-layer).

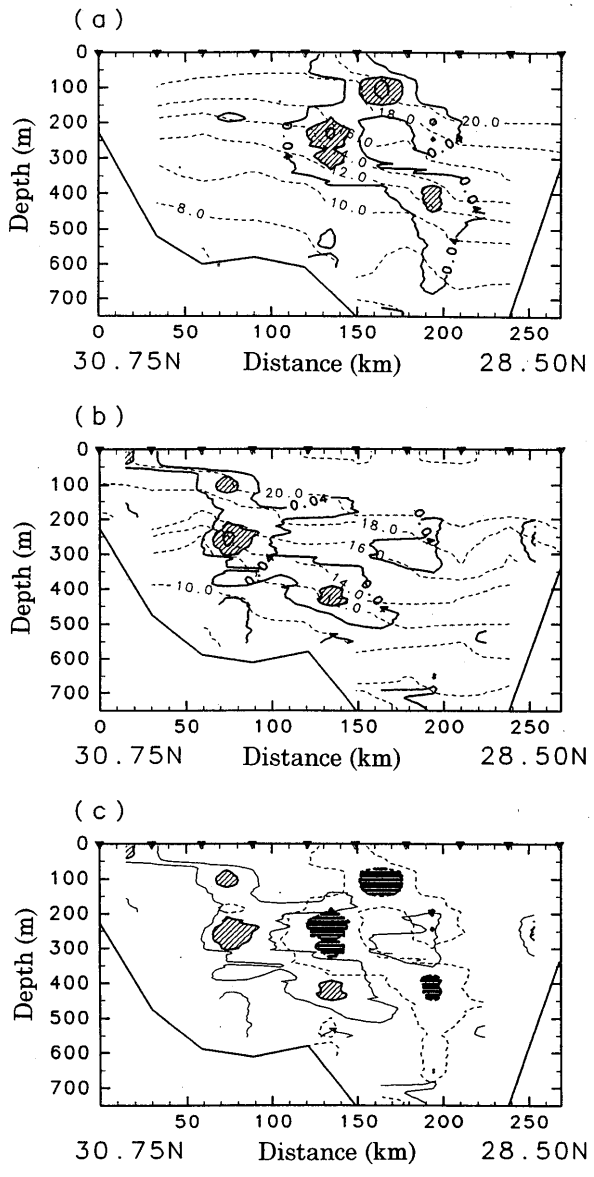

Fig. 10 Cross-sections of horizontal temperature gradient (solid line) along line C (a) in leg. 1 and (b) in leg. 2. Contour interval is 0.04℃/m. Hatched area indicates horizontal temperature gradient larger than 0.08℃/m. Temperature distribution (dashed line) is superimposed in (a) and (b). Contour interval is 2.0℃. (c) Horizontal temperature gradients in leg. 1 (dashed line) and leg. 2 (solid line).

In order to clarify the change of the baroclinic structure, the change of horizontal temperature gradients are examined. Figures 10a and 10b show the distributions of horizontal temperature gradients in leg. 1 and leg. 2, respectively. Maximums of the horizontal temperature gradient larger than 0.08℃/m are hatched. In the cross-section of leg. 1 (Fig. 10a), two areas with the large horizontal temperature gradient (≥0.04℃/m) exist; one is located near the outcropped area of the upper-interface (18-20℃ isotherms) which corresponds to the Kuroshio front, and the other on the lower-interface (12-16℃ isotherms). Such distributions of the horizontal temperature gradient are confirmed in leg. 2 (Fig. 10b), although the horizontal temperature gradient near the outcropped area of the upper-interface was weakened due to the horizontal extension of the upper-layer. Horizontal shifts of maximums of the horizontal temperature gradient are examined in Fig. 10c. Two maximums hatched at 250-m and 400-m depths on the lower-interface shifted northward (about 60km) without changing the distance between them. On the other hand, the uppermost maximum at 100-m depth on the upper-interface changed the relative place to the maximum at 250-m depth on the lower-interface from its south to a little north. These indicate that the structure of the lower-interface changed little during the northward migration of the Kuroshio, while that of the upper-

interface changed significantly.

The ADCP surface velocity is analyzed in the connection with the horizontal temperature gradient, because the horizontal temperature gradient represents the vertical shear of the geostrophic velocity based on the thermal wind relation. Normal components of the surface ADCP velocity to line C (Fig. 7c as leg. 1 and Fig. 8c as leg. 2) show two velocity maximums regarded as the Kuroshio axis. The northern Kuroshio axis geographically corresponds to the northern maximum of the horizontal temperature gradient on the lower-interface in both leg. 1 and leg. 2. On the other hand, the southern one geographically corresponds to the maximum of the horizontal temperature gradient on the upper-interface in leg. 1, but not in leg. 2. The maximum of the horizontal temperature gradient on the upper-interface in leg. 2 was weakened and moved toward the position of the northern Kuroshio axis, and this probably resulted in weakening the surface velocity at the southern Kuroshio axis in leg. 2. It is inferred that the baroclinic velocity structure at the northern Kuroshio axis was maintained because the lower-interface changed little, while that at the southern one was remarkably weakened by the significant change of the upper-interface.

Summary

The relationship between the variation of the position of the Kuroshio axis and that of the Kuroshio front has been examined by analyzing short-term changes of temperature and current cross-sections. The position of the Kuroshio axis has been determined by the maximum ADCP velocity at 5-m depth perpendicular to each line. The Kuroshio front has been determined by the outcropped line of 20℃ isotherm. The outcropped line of 20℃ isotherm had a good correspondence to the on-shore edge of the subsurface warm water of the Kuroshio.

On the southern line across the continental slope (line A), the displacement of the Kuroshio front (~57km/3.5days) was about 7 times larger than that of the Kuroshio axis (~8km/3.5days). On the northern line across the continental slope (line B), the displacement of the kuroshio front (~35km/5days) was about 1.8 times larger than that of the Kuroshio axis (~20km/5days). On both line A and line B, the water-mass front between the Kuroshio water and the shelf water, which was identified by 16-19℃ isotherms, did not move. On the Tokara Strait (line C), the displacement of the Kuroshio front (~118km/8days) was about twice larger than that of the Kuroshio axis (~59km / 8days). Horizontal shifts of the position of the Kuroshio front are closely related to those of the Kuroshio axis in all cross-sections. However, the former varied with a several times (1.8~7) larger amplitude than the latter.

The relationship mentioned above has been examined in the Tokara Strait precisely, focusing on the change of the baroclinic structure caused by the northward migration of the Kuroshio. The Kuroshio in the Tokara Strait was vertically separated into three layers by two interfaces with the large vertical temperature gradient: i.e., the upper-interface (18-20 ℃ isotherms) and the lower-interface (12-14 ℃ isotherms in the southern strait while 14-16℃ isotherms in the northern strait) within the main thermocline. The outcropped area of the upper-interface corresponded to the position of the Kuroshio front. The Kuroshio in the Tokara Strait had two current axes. The velocity structure at the

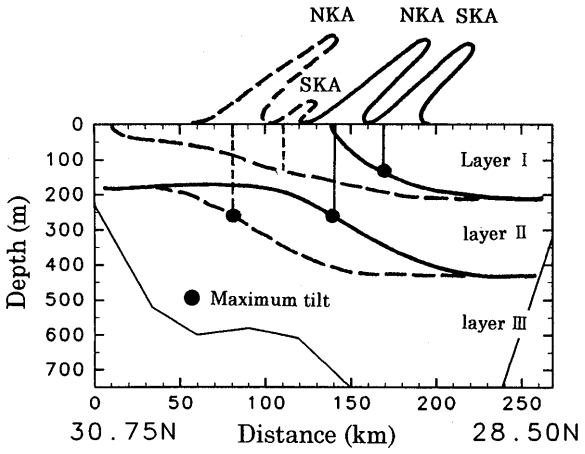

Fig. 11 The schematic view of the baroclinic structure change between leg. 1 (solid line) and leg. 2 (dashed line) in the Tokara Strait. The northern and southern Kuroshio axes are indicated by NKA and SKA in the figure, respectively.

northern Kuroshio axis was related to the horizontal shear of the lower-interface, while that at the southern one the upper-interface. The horizontal structure of the lower-interface changed little during the northward migration of the Kuroshio, while that of the upper-interface changed significantly. This probably resulted in the maintained velocity at the northern Kuroshio axis and the weakened velocity at the southern Kuroshio axis. The temporal change of the baroclinic structure in the Tokara Strait is schematically drawn in Fig. 11. The weakened tilt of the upper-interface during the northward migration of the Kuroshio, indicates that the available potential energy in the upper and middle layers was released. This suggests that a mechanism generating the Kuroshio front fluctuation is the baroclinic instability. On the other hand, the fact that the tilt of the lower-interface changed little, suggests that the meandering of the Kuroshio axis is generated by the other mechanisms. It is inferred that the evolution of the upper-interface is dynamically different from that of the lower-interface. The further studies based on the dynamic model will be needed to clarify mechanisms of the Kuroshio axis and front fluctuations.

Acknowledgments

Data used in this study were obtained in the KE96-14 cruise by T/V Keitenmaru during March 1-10, 1997. We thank crews of the Keitenmaru and Mr. S. Fujieda for their help collecting data, and also thank students of the Physical Oceanography Group, Kagoshima University for their work in observation. We greatly thank the late captain of T / V Keitenmaru, Prof. Y. Yuwaki. who supported our observation broadly. A part of this study was supported by the International Cooperative Research Programme on Global Ocean Observing System (GOOS) through Prof. S. Imawaki of Kyushu University.

References

1) T. Yamashiro, A. Maeda and M. Sakurai (1993): Mean position and deviation of the Kuroshio axis in the East China Sea. *Umi to Sora*, **69**, 125-134. (in Japanese with English abstract and legends)

2) T. Yamashiro and M. Kawabe (1996): Monitoring of position of the Kuroshio axis in the Tokara Strait using sea level data. *J. Oceanogr.*, **52**, 675-687.

3) B. Qiu, T. Toba and N. Imasato (1990): On the Kuroshio front fluctuations in the East China Sea using satellite and in situ observational data. *J. Geophys. Res.*, **95**, 18191-18204.

4) H. Akiyama and T. Ameya (1991): Variation in the Kuroshio front around the Tokara Strait. *Umi to Sora*, **67**, 113-132. (in Japanese with English abstract and legends)

5) A. Maeda, T. Yamashiro and M. Sakurai (1993): Fluctuation in volume transport distribution accompanied by the Kuroshio front migration in the Tokara Strait. *J. Oceanogr.*, **49**, 231-245.